Topological and geometrical properties of crack patterns produced by the thermal shock in ceramics

W. Korneta,* S. K. Mendiratta,† and J. Menteiro
Departamento de Fisica, Universidade de Aveiro, 3800 Aveiro, Portugal
(Received 13 June 1997)

We study the crack patterns produced by thermal shock in ceramic tableware. Cracks produced at sufficiently high-temperature gradients partition the surface plane of a ceramic material into cells forming a random two-dimensional space-filling cellular structure. The topological and geometrical properties of these structures are described and analyzed. The distribution of the number of cell sides, the topological correlations between adjoining cells, the probability distributions of a cell area and side length, the average area and perimeter of n-sided cells, and the distribution of vertex angles are determined. The results show that the studied cellular structures obey the Aboav-Weaire law [Metallography **3**, 383 (1970); **7**, 157 (1974)] and Desch's law [J. Inst. Metals **22**, 241 (1919)]. The scaling behavior of cellular structures obtained at different temperature gradients of the thermal shock is also presented. [S1063-651X(98)00803-4]

PACS number(s): 62.20.Mk, 05.90.+m, 44.90.+c, 46.30.Nz

I. INTRODUCTION

The susceptibility of ceramic materials to failure due to thermal stresses is one of the factors limiting their applications. The thermal stresses result from temperature gradients within a body and the fact that free expansion or contraction of each volume element of a body cannot occur. The effect of thermal stresses on ceramic materials depends on the stress level, the stress distribution, and the material characteristics such as homogeneity, porosity, and existing cracks. When ceramic materials are subject to a rapid change in a temperature (thermal shock), substantial thermal stresses develop which may cause the formation of cracks and eventual fracture of a material. The critical temperature difference ΔT_c for the initiation of severe damage is used as the descriptive parameter for the thermal shock resistivity of ceramics; ΔT_c is usually determined by the significant drop in material strength and it is also indicated by the appearance of cracks. In the thermal shock the main source of stress intensification comes from the temperature gradient along the heat flow axis. Moreover, thermal stresses are largest at the surface. The most probable cracks that form, therefore, during the thermal shock are thus surface cracks normal to the surface. These cracks do not form a barrier for the heat flow. In the direction perpendicular to the surface they can be well characterized by their penetration depths. More interesting is the crack pattern on the surface. This pattern consists of loops that partition the surface plane into cells and also of dangling branches in larger cells. The random space-filling cellular patterns associated with stress-relief cracking are common in nature, e.g., cooling-induced patterns in lava flows and shrinkage crack patterns in mud (see Ref. [1] and references therein). In fact, random cellular structures can be observed in many natural phenomena and it was emphasized by various authors that these structures abound in nature (see the review papers of Weaire and Rivier [1] and Stavans [2] for many examples). In recent years the topological and geometrical properties of such structures have been studied intensively, both experimentally and theoretically, and the methods to classify them have been proposed. The semiempirical laws generally obeyed in different random cellular structures have been formulated. Attempts have been made to derive these widely observed empirical laws by methods of statistical mechanics [3]. Recent results obtained within mean-field theories, Potts model simulations, and Monte Carlo studies [1,2] have also contributed to the basic understanding of cellular structures.

The aim of this paper is to present topological and geometrical properties of random cellular structures formed by cracks produced by the thermal shock in commercial ceramic materials used to make common dinner plates; the unglazed plates were supplied by Sociedade Porcelana Alcobaça Lda. (SPAL), Portugal. Our interest in this subject comes from the fact that understanding and control of crack propagation during the thermal shock in ceramic products is technologically important. We describe regularities that we found in the organization of cracks induced by the thermal shock and we compare patterns formed by these cracks with patterns observed in other random cellular structures of many natural phenomena. We also consider the effect of the temperature gradient on topological and geometrical properties of created crack patterns.

II. EXPERIMENTAL PROCEDURE

The disk-shaped samples having a diameter of 15 mm and thickness of 4.5 mm were core drilled from the central part of unglazed plates. One of the most widely used thermal shock tests of ceramic materials is the classical water quench test. We performed the water quench test using a specially designed apparatus [4] that guaranteed a repeatable and mea-

*Permanent address: Faculty of Physics, Technical University, Malczewskiego 29, 26-600 Radom, Poland.
†Author to whom correspondence should be addressed. Electronic address: skm@fis.ua.pt

surable thermal gradient. In our experiments the test sample was allowed to equilibrate in a vertical electrical furnace for 20 min and dropped in a time shorter than 1 s into a water bath having the temperature 20 °C. During the water quench the increase of the bath temperature never exceeded 1 °C. In a dry run it was confirmed that the temperature of the sample, as measured at the surface, at the moment of hitting the cold water was not lower than few degrees from that in the furnace. Since the whole procedure is automatic, this small drop is always repeatable. Subsequently, the sample were taken out of the bath, dried, and covered with 1% water solution of methylene blue powder supplied by MERCK. The painted samples were left for drying and the excess ink was removed by water. This procedure rendered cracks visible. The critical temperature difference ΔT_c was determined as the quenching temperature difference in which a pronounced drop in the retained bending strength (measured in a standard three-point-bending test) was observed [4]. We obtained $\Delta T_c \approx 200$ °C, corresponding to the initial temperature 220 °C in the water quench test. We noticed that for the temperature gradient $\Delta T < \Delta T_c$, the crack pattern did not appear. Using the image scanner, we digitized images of visible crack patterns at 703×703 pixel resolution and eight bits of gray scale. The standard image processing operations were used to enhance the contrast of crack patterns. A binary image was then derived from the gray scale image using a thresholding routine. Finally, the thinning binary morphological operation that thins objects to lines and preserves the Euler number was applied to the binary image. The skeleton thus obtained contains both the topological and the metric information of the crack structure and is suitable for measurement operations. In order to verify the correspondence between a crack pattern and its skeleton we always superimposed the skeleton on the original gray scale image. Three examples of the obtained crack patterns with their superimposed skeletons are shown in Figs. 1 and 2. One can see how the crack pattern changes when the temperature gradient in the water quench test increases. The skeleton of the crack pattern after removal of all dangling branches forms a random two-dimensional cellular structure in which cells are separated by very thin boundaries and they completely fill the space. An example of such a structure is shown in Fig. 1. Though the structure of dangling bonds and the depth distribution of cracks also carry useful information about the physics behind the phenomenon, we limit ourselves in this paper to the study of closed loop surface cracks.

In the crack patterns produced at temperature gradients larger than but close to ΔT_c one could distinguish only a few cells; therefore, our analysis was performed only for crack patterns produced at higher temperature gradients where the proportion of inner cells to all cells was higher than 0.5. We choose the following initial temperatures of the water quench test: 300 °C, 350 °C, 400 °C, 600 °C, and 700 °C. All the quenches were done approximately for the same time, i.e., under 1 s. The proportion of the number of inner cells to the number of cells at the boundary of a sample varied approximately from 1.4 (300 °C) to 5 (700 °C). The number of samples taken into account was the following: 11 (300 °C), 7 (350 °C and 400 °C), and 2 (600 °C and 700 °C). The results presented below were obtained by averaging the data over the samples.

III. TOPOLOGICAL PROPERTIES

In this section we discuss the general topological features of the crack loops. Special attention is paid to the topological correlation between neighboring cells.

A. Distribution of topological parameters

In two-dimensional cellular structures the topology of a cell can be described by only one parameter, i.e., the number n of sides of a cell. The number n in random cellular structure is a topological random variable and can be characterized by the discrete probability distribution function $P(n)$ and its moments. Both the $P(n)$ and its moments are the most frequently measured experimental data and they attracted the greatest attention in the theoretical studies of random cellular structures. In Fig. 3 we present distributions $P(n)$ determined in our cellular structures. The typical error bars are also shown in this figure. One can notice that within experimental accuracy it is difficult to distinguish probability distributions $P(n)$ obtained in cellular structures corresponding to different temperature gradients of the thermal shock. One characteristic feature of our cellular structures that follows from Fig. 3 is that the probability of finding cells with five or six sides is very large, the value for six being higher. A significant occurrence of pentagons along with the most expected hexagons was also observed in crack patterns formed in cooling basalt flows and other contracting systems (see Ref. [5] and references therein). The probability distributions shown in Fig. 3 have maxima for n between 5 and 6, they are asymmetric, and the relation $P(5) > P(7)$ is satisfied. These properties of $P(n)$ have been observed also in other random cellular structures. The probability distribution can be characterized by its moments. In the experimental and theoretical studies of random cellular structures usually only the first moment $\langle n \rangle$, which determines the position of the center of gravity of the distribution, and the second moment μ_2, which determines the dispersion of n values around the mean, are considered. Higher moments of $P(n)$ are sensitive to the large values of n, which is hard to measure because there are only a few large cells. They are useful only as qualitative indicators, e.g., the third moment measures the asymmetry of the distribution. Analyzing random cellular structures representing crack patterns, we observed that the vertices are predominantly trivalent. There were only a few tetravalent vertices (about 1%). This small percentage may be due to the resolution of images of crack patterns. The number of cells, edges, and vertices of any cellular structure obeys the conservation law, i.e., Euler's relation [1]. The consequence of Euler's relation for the infinite two-dimensional cellular structures with only trivalent vertices is that the average number of sides of a cell in such a structure is 6, i.e., $\langle n \rangle = 6$. In finite cellular structures $\langle n \rangle$ and the deviation from 6 increases when the number of cells decreases. This effect was observed, e.g., in two-dimensional soap froth [6] and Voronoi diagrams [7]. We obtained the following values for $\langle n \rangle$ averaged over crack patterns produced at the same initial temperature of the water quench test: 5.93 (for 700 °C, 600 °C, and 400 °C), 5.86 (for 350 °C), and 5.79 (for 300 °C). The variance μ_2 of $P(n)$ shows a great diversity of values in different natural random cellular structures. It is of the order of unity for biological

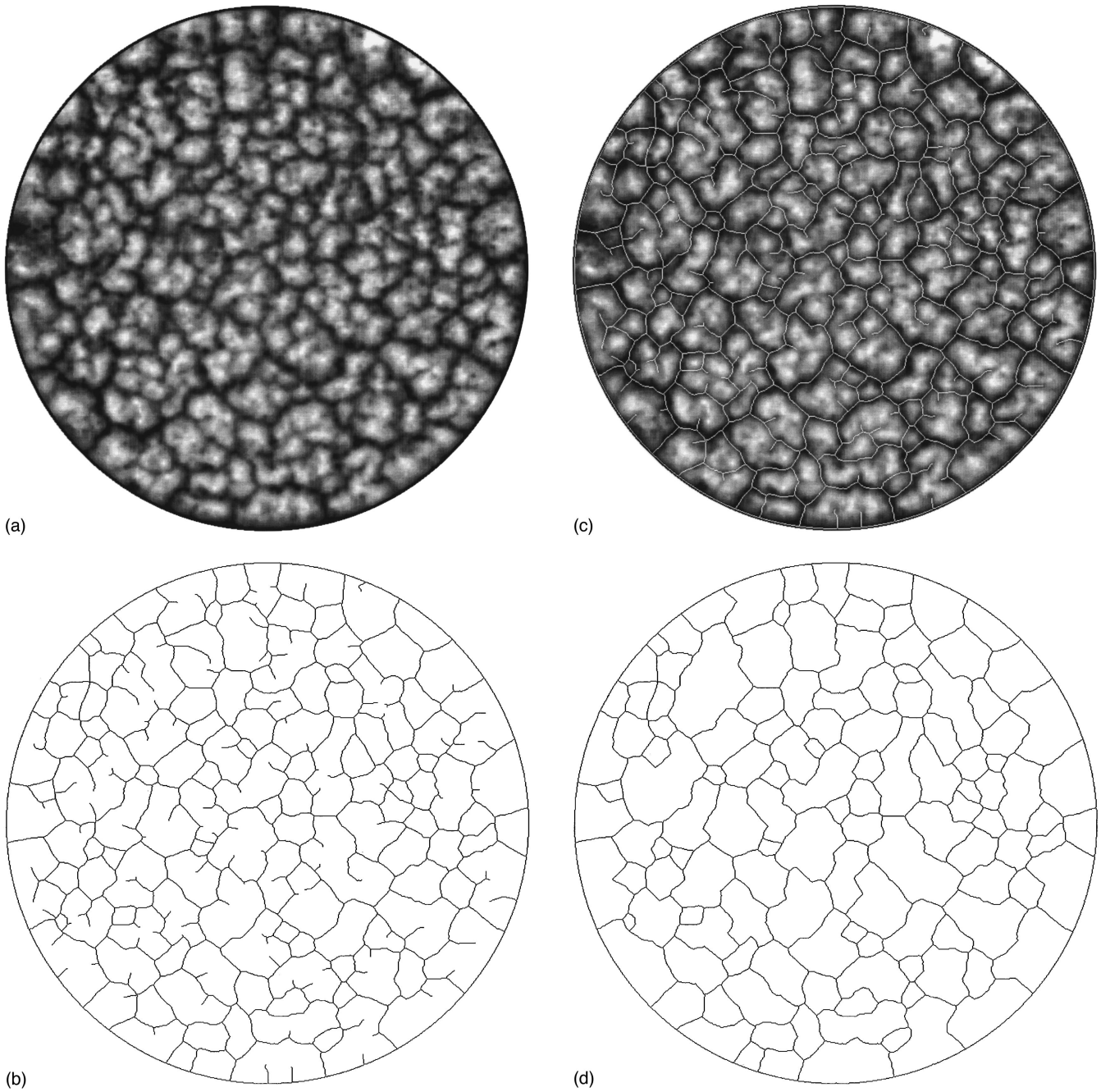

FIG. 1. Crack pattern produced by the thermal shock in ceramic material and its skeleton. The initial temperature in the water quench test was 400 °C. (a) The original gray scale image, (b) the skeleton, (c) the skeleton superimposed on the original, and (d) the skeleton after removal of dangling branches.

cells [8] and lies between 1 and 3 for soaps froths [6,9]. The second moments of probability distributions shown in Fig. 3 are the following: 2.67 (700 °C), 2.70 (600 °C), 2.82 (400 °C), 2.81 (350 °C), and 2.74 (300 °C), i.e., they are in the range $\mu_2 = 2.75 \pm 0.07$.

B. The Aboav-Weaire law

The semiempirical Aboav-Weaire law [2,10,11] is the most frequently obeyed empirical regularity observed in random cellular patterns. It describes topological correlation between neighboring cells. Let $m(n)$ be the average number of sides of cells surrounding an n-sided cell. Aboav [10] observed empirically that in cellular structures with trivalent vertices $m(n)$ is linearly related to $1/n$. The Aboav-Weaire law is usually expressed by the equation

$$nm(n) = (6-a)n + (6a+\mu_2), \tag{1}$$

where a is a parameter and μ_2 is the variance of $P(n)$. In many natural random cellular structures the parameter a is of the order of 1 [6,8] and does not exceed 2 [12]. In finite cellular structures one should replace 6 in Eq. (1) by $\langle n \rangle$ [12]. Peshkin *et al.* [13] showed that the linearity implied by the Aboav-Weaire relation can be explained by the maximum-entropy principle with constraints imposed on

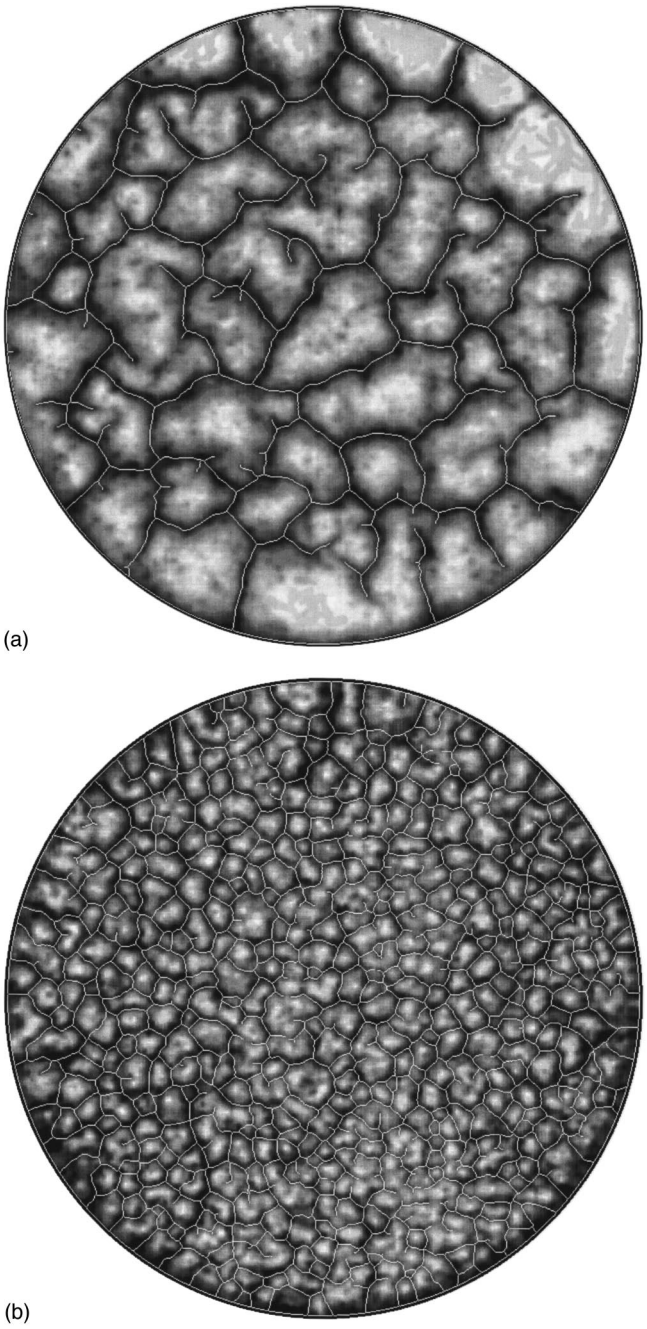

FIG. 2. Gray scale images of crack patterns produced by the thermal shock in ceramic material with superimposed skeletons of cracks. The initial temperature in the water quench test was (a) 300 °C and (b) 700 °C.

possible distributions $P(n)$ and $M_n(k)$, where $M_n(k)$ is the average number of k-sided cells adjoining an n-sided cell. In Fig. 4 we show experimentally measured dependences of $nm(n)$ on n obtained for cellular structures corresponding to crack patterns produced by the thermal shock at different temperature gradients. The data for this figure were obtained by calculating $m(n)$ only for the inner n-sided cells. We also plotted, for comparison, the straight line given by Eq. (1) with $a=1$ and $\mu_2=2.75$. The experimental data follow, in general, the Aboav-Weaire law very well. There is a slight departure for cells with more than nine sides, which may be due to the fact that the number of data points for many-sided cells is low.

C. Two-cell topological correlations

In this section we describe topological correlations between shapes of nearest-neighbor cells more precisely than it is expressed by the Aboav-Weaire law. The probability $P_n(k)$ of finding k-sided cell in the neighborhood of an n-sided cell equals $M_n(k)/\Sigma_k M_n(k)$, where $M_n(k)$ has been defined above. The topological correlation functions $C(n,k)$ studied in this section are defined as $C(n,k)=P_n(k)/P(k)$. They express the proportion of the probability of finding k-sided cells in the neighborhood of n-sided cells to the probability of finding k-sided cells anywhere in random cellular structure. The correlation functions $C(n,k)$ defined above differ from the correlation functions studied, e.g., in Refs. [7,12,14] by the factor $1/n$, because the sum of quantities $M_n(k)$ over k is n [13]. The correlation functions $C(n,k)$ have been less investigated in cellular structures than the probability distribution $P(n)$ or the Aboav-Weaire relation. These functions have drawn the attention in recent years because they allow a comparison of topological properties of cellular structures with different distributions $P(n)$. Comparing the topological correlations in different random cellular structures, one observes their restricted variability in structures that have similar values of the variance μ_2. Moreover, these correlations undergo a regular and smooth change when μ_2 increases. The correlations $C(n,k)$ in random cellular structures are found not to depend on the scale and physical phenomena in which they occur. The observed dependence of correlations $C(n,k)$ on k is usually tested with the linear dependence [14]

$$C(n,k)=1+\frac{1-(a/\mu_2)(n-6)}{n}(k-6), \qquad (2)$$

where a is the parameter of the Aboav-Weaire law and μ_2 is the variance of $P(n)$. One should notice that the correlations $C(n,k)$ are in fact determined by a single structural parameter a/μ_2. Figure 5 shows the dependence of the correlations $C(n,k)$ on k, which we obtained for random cellular structures formed by cracks produced by the thermal shock at different temperature gradients. These data were obtained by taking into account only the inner n-sided cells. The conclusion that follows from our data is that the number of sides of adjoining cells are correlated: many sided cells have few-sided neighbors and vice versa. The probability of selecting six-sided cells in the neighborhood of a cell with any number of sides is the same, i.e., six-sided cells are homogeneously distributed among other cells in our cellular structures. This also agrees qualitatively with the peak of $P(n)$ in Fig. 3, which is close to 6. If the number n of cell sides increases from 4 to 8, the probability of selecting a cell with any number of sides in its neighborhood tends to the probability of selecting this cell randomly in the structure. In Fig. 5 we have also plotted the straight lines according to Eq. (2) with $a=1$ and $\mu_2=2.75$. One can notice a reasonable agreement between our experimental data and relation (2). The devia-

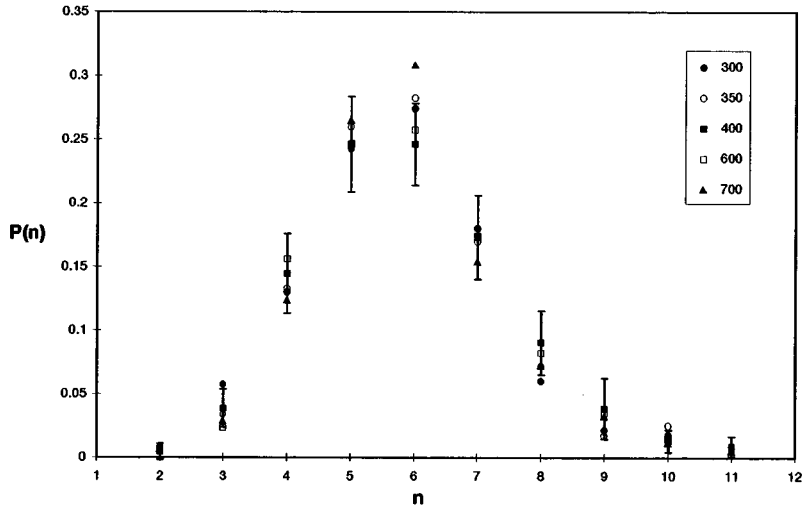

FIG. 3. Distribution $P(n)$ of the number n of sides of cells in random cellular structures formed by cracks produced by the thermal shock in ceramic material. The initial temperatures in the water quench test are indicated. The error bars denote a standard deviation and they are given for the initial temperature 400 °C.

tions from this relation for the smallest and the largest k values can be due to the too small number of cells with the extreme number of sides. The deviations are also larger for correlations in cellular structures corresponding to the smaller temperature gradients of the thermal shock because the number of cells becomes lower. The topological correlations $C(n,k)$ must fulfill the condition $C(n,k) \geqslant 0$ for all k and n. Formula (2) gives unphysically $C(4,k) < 0$ for $k \leqslant 4$, so it cannot be used to describe topological correlations between the smallest cells. In our structures we obtained $C(3,3) = 0$; the same has been observed in cellular structures [12,14]. Indeed, this relation follows from the general topological constraint that a cell does not share two edges with any one of its neighbors.

IV. METRIC PROPERTIES

There are several metric parameters of a cell whose probability distributions can be used to characterize cellular structures, e.g., the area, perimeter, side length, radius of gyration, equivalent diameter of a cell, or segments into which straight lines whose directions are random are broken by their intersections with cell sides. Among these parameters the probability distributions of cell areas and side lengths are the most often reported [1,2,9,15–19] in cellular systems. In general, one expects that all lengths should behave in a similar way and the area should go as their square [15]. The probability density functions of cell areas A normalized by the median cell area A_{med} in cellular structures formed by cracks produced by the thermal shock at different tempera-

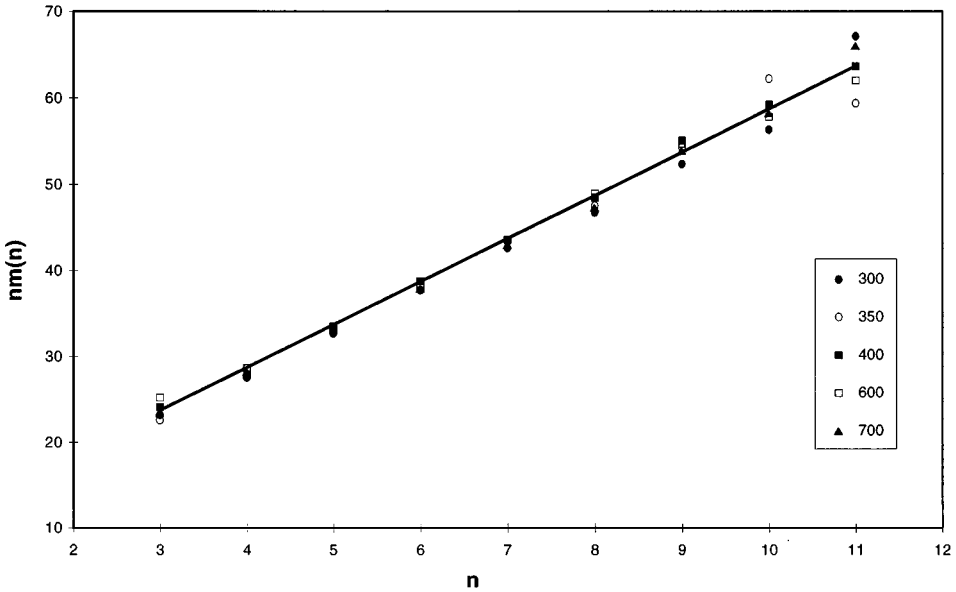

FIG. 4. Aboav-Weaire law: the average correlation $nm(n)$ as a function of n. $m(n)$ is the average number of sides of the nearest-neighbor cells adjacent to n-sided cells. The straight line is calculated from Eq. (1) with $a = 1$ and $\mu_2 = 2.75$. The initial temperatures in the water quench test are indicated.

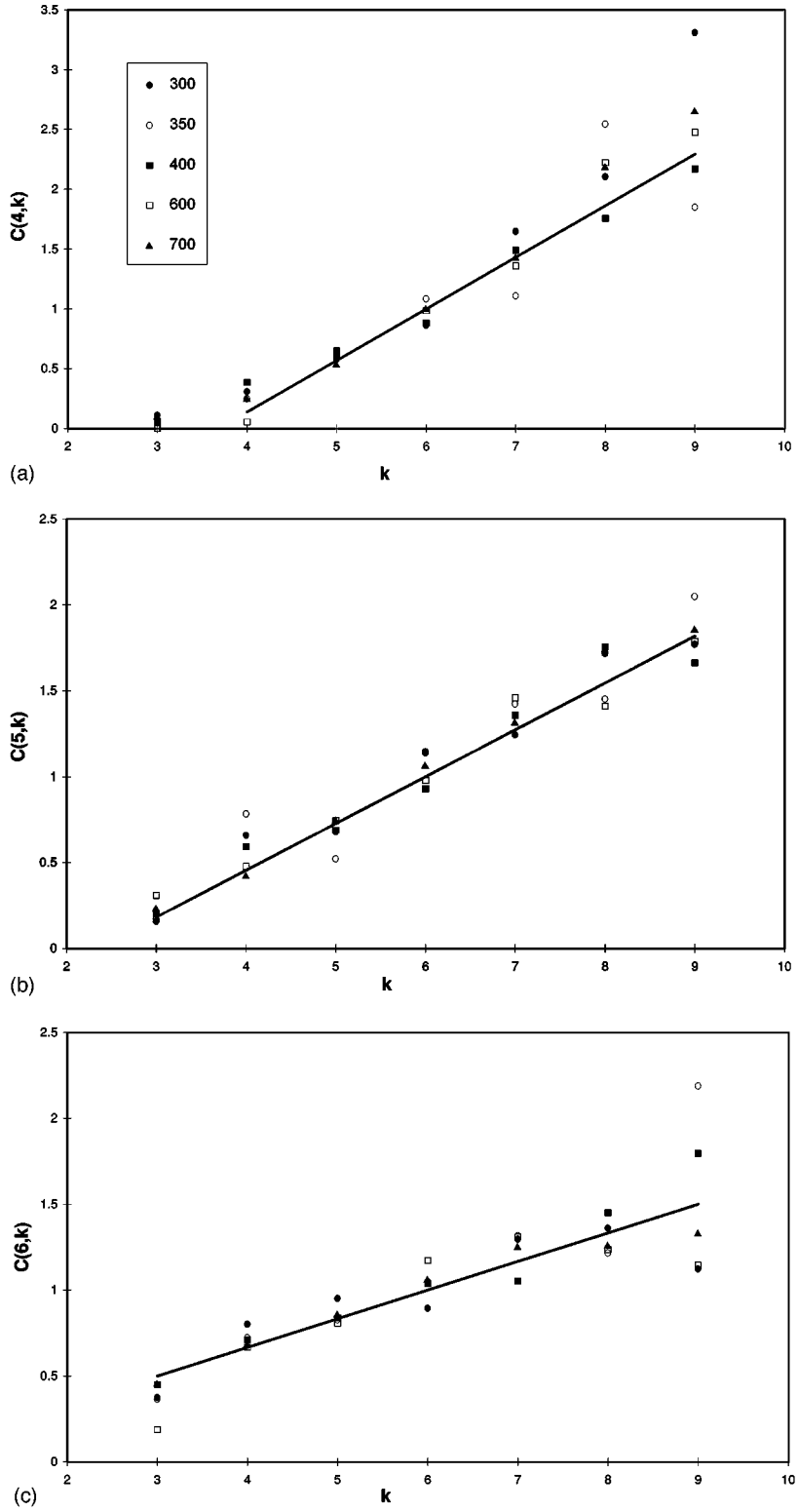

FIG. 5. Topological two-cell correlations $C(n,k)$ defined as the proportion of the probability of finding k-sided cells in the neighborhood of n-sided cells to the probability of finding k-sided cells anywhere in the cellular structure. The straight lines are calculated from formula (2) with $a=1$ and $\mu_2=2.75$. The initial temperatures in the water quench test are indicated.

ture gradients are shown in Fig. 6. In Fig. 7 we present the probability density functions of side lengths L (along cracks), normalized by the median side length L_{med} obtained in the same cellular structures as in Fig. 6. One can notice that the probability density functions corresponding to different temperature gradients of the thermal shock within experimental error are the same. We conclude that there exist scale invariant probability density functions that describe distributions of areas and side lengths in all our random cellular structures. Other similarities between cellular structures pro-

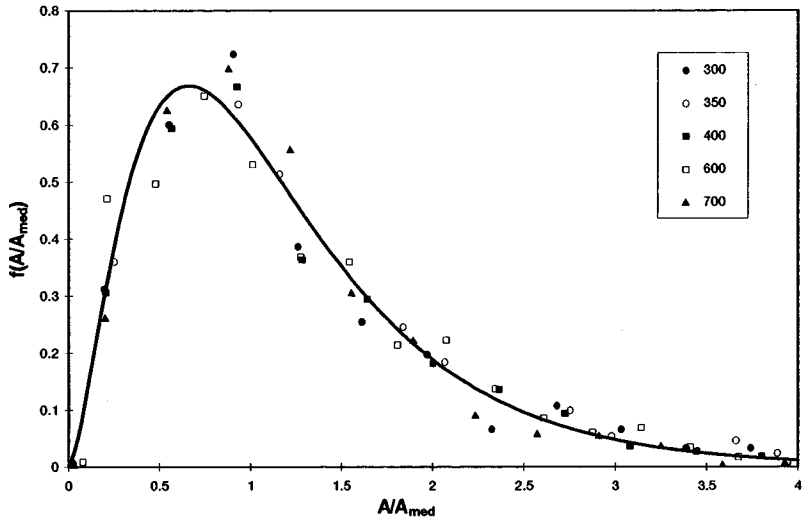

FIG. 6. Probability density function of normalized cell areas in random cellular structures formed by cracks produced by the thermal shock in ceramic material. The curve results from a fit of the probability density function given by Eq. (3) to experimental data. The initial temperatures in the water quench test are indicated.

duced by the thermal shock at different temperature gradients arise from relations between average quantities. We obtained for all temperature gradients the following ratios of average quantities: $\langle P\rangle/\langle L\rangle = 5.80 \pm 0.10$ (P denotes the perimeter of a cell), $\langle A\rangle/\langle L\rangle^2 = 1.91 \pm 0.14$, and $\langle A\rangle/\langle L_E\rangle^2 = 2.48 \pm 0.05$ (L_E is the Euclidean side length of a cell). In a regular hexagonal structure $\langle P\rangle/\langle L\rangle = 6$ and $\langle A\rangle/\langle L_E\rangle^2 \approx 2.56$. The experimental values obtained here indicate strong correlations between the area, perimeter, and side lengths in our cellular structures. There are no exact results for the form of probability density functions for the area and side length in random cellular structures and several functions have been proposed. In Ref. [15] one can find four different probability density functions proposed to fit the experimental data. The most often used function was γ distribution because it gives a good fit to the distribution of areas in Voronoi networks [18,19] and the lognormal distribution because it results from multiplicative random events. We have tried to fit different probability density functions to our experimental data. The goodness of fit was characterized by χ^2 test. The smallest test statistics χ^2 was obtained for the probability density function

$$f(x) = \frac{\alpha x^{\alpha-1}}{\sigma\sqrt{2\pi}} \exp\left(-\frac{(x^{\alpha}-\mu)^2}{2\sigma^2}\right), \tag{3}$$

where α, μ, and σ are parameters. This function has been used often to describe the distribution of grain sizes in polycrystals (see Ref. [20] and references therein). It was demonstrated [20] that the distribution of grain sizes in polycrystalline ceramics is the most accurately represented by the

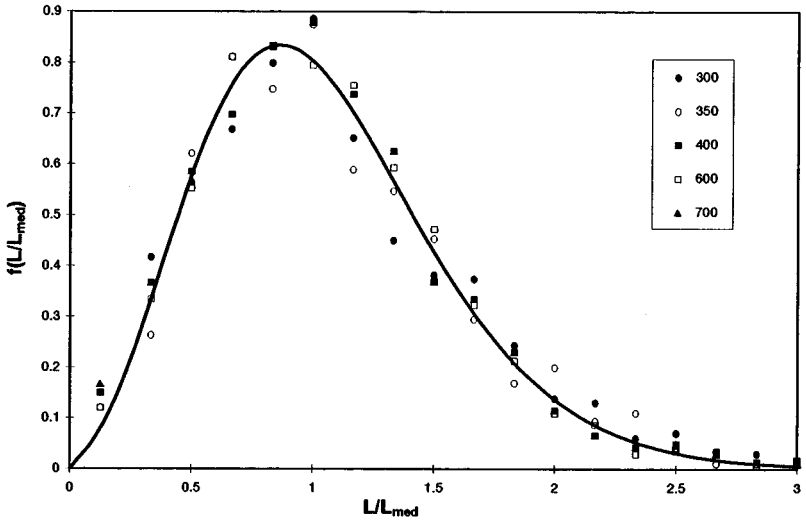

FIG. 7. Probability density function of normalized cell side lengths in random cellular structures formed by cracks produced by the thermal shock in ceramic material. The curve results from a fit of the probability density function given by Eq. (3) to experimental data. The initial temperatures in the water quench test are indicated.

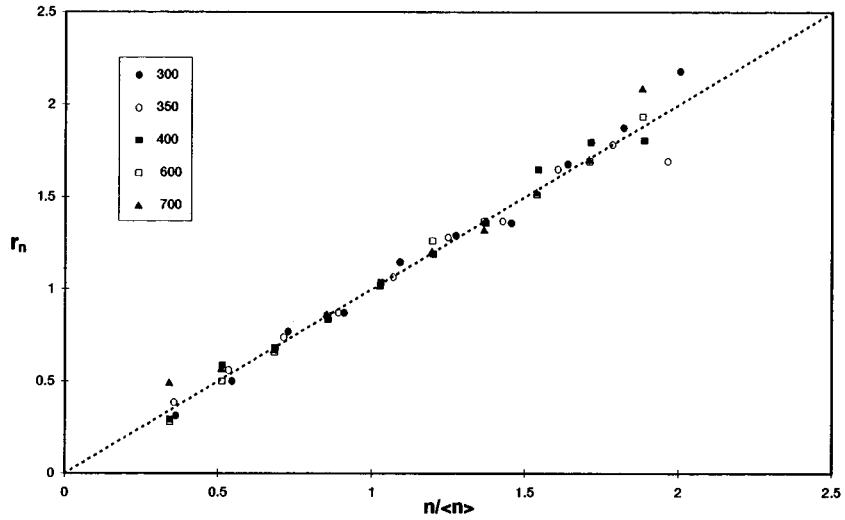

FIG. 8. Radius law: the normalized average radius of n-sided cells as a function of the normalized number of cell sides. The initial temperatures in the water quench test are indicated.

function (3) and it does not depend on the average grain size. We obtained the following parameters: $\alpha_A=0.25$, $\mu_A=1$, and $\sigma_A=0.17$ for the distribution of A/A_{med} and $\alpha_L=0.5$, $\mu_L=1$, and $\sigma_L=0.25$ for the distribution of L/L_{med}. The results of the fit are shown in Figs. 6 and 7. The relation between parameters $\alpha_L=2\alpha_A$ indicates that the area behaves approximately as a square of the side length, as expected. There is thus a correlation between the distribution laws for areas and side lengths in our cellular structures. The similar correlation was also observed in Voronoi mosaics where the shifted γ law was used to fit the area and side length distributions [15].

V. THE RADIUS LAW

In this section we consider relations between topological and metric parameters in our random cellular structures. The correlation between the shape and size of cells in random cellular structures attracted the attention of scientists a long time ago [21,22]. The two relations were discovered empirically: Lewis's law and Desch's law, also known as the radius law. Lewis's law relates the average area of n-sided cells linearly to n, whereas Desch's law relates the average radius (defined as the square root of an area) of n-sided cells linearly to n. These two laws are obeyed by a wide variety of random space-filling model structures and experimental systems (see the paper of Glazier *et al.* [9] and references therein). The Lewis's and Desch's laws can thus be used to classify random two-dimensional cellular structures. Rivier [3] used the maximum-entropy principle to prove these laws theoretically. Rivier's maximum-entropy method was based on the observation that random cellular structures are usually indistinguishable apart from the scale of measurement. It is thus improbable that specific forces are responsible for the universal properties of random cellular structures. An ''ideal'' random space-filling structure can thus be determined by mathematical constraints only and the fact that the structure is the most probable one. This structure obeys Lewis's law. In many systems all the energy is carried by boundaries between cells so the average energy, proportional to the perimeter of a cell, is the different physical constraint in these systems. Entropy maximization under the inescapable mathematical constraints and this physical constraint yields the radius law.

Let r_n denote the normalized average radius of n-sided cells defined as $r_n=\langle\sqrt{A_n}\rangle/\langle\sqrt{A}\rangle$, where A_n is the area of n-sided cells [9]. In Fig. 8 we show r_n as a function of n in our random cellular structures formed by cracks produced by the thermal shock at different temperature gradients. In this figure only the inner cells in a structure were taken into account. One can notice that the dependence of r_n on n is linear for all temperature gradients, indicating that our random cellular structures obey Desch's universal law. The random cellular structures formed by cracks thus belong to the class of random space-filling structures in which the energy associated with cell boundaries (cracks) is probably the important mechanism in the development of the structure.

In the natural cellular structures fewer experimental results have been presented for correlations between other metric parameters such as the average perimeter or side length of n-sided cells and the topological parameter n. These correlations were experimentally studied in vegetable tissues [8] and the linear relationship between the average perimeter of n-sided cells and n was obtained. In our investigations the perimeters of the cells are very important because they represent cracks. Figure 9 shows the average perimeter of n-sided cells as a function of n for all our cellular structures. The data corresponding to different temperature gradients of the thermal shock overlap after normalization shown in the figure. The dependence of the average perimeter of n-sided cells on n is linear for $n<9$. The deviation from this linear dependence for large cells indicates that these cells are more elongated than smaller cells. This may be due to the presence of dangling branches in large cells that failed to connect cell sides.

VI. DISTRIBUTION OF VERTEX ANGLES

The variation of the angle between cell sides at vertices has been little studied in random cellular structures. This is

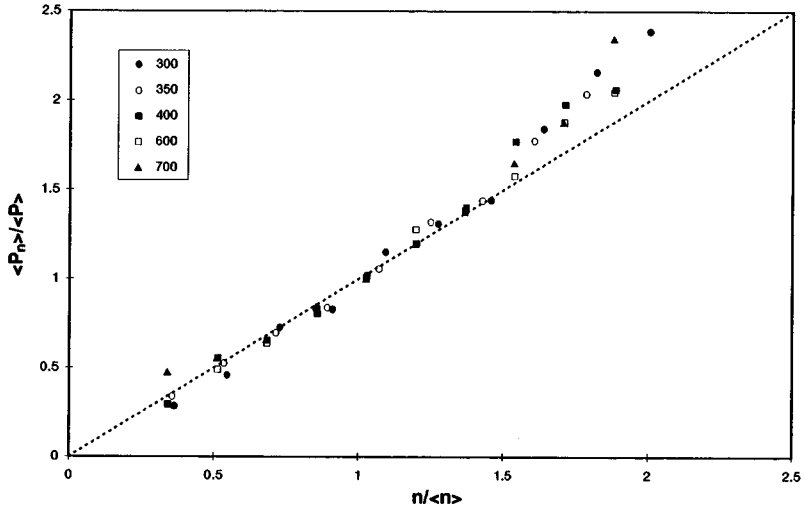

FIG. 9. Normalized average perimeter of n-sided cells as a function of the normalized number of cell sides. The initial temperatures in the water quench test are indicated.

due to the observation that in many natural trivalent cellular space-filling structures the angle between cell sides at vertices is tightly distributed around 120° [1]. This property also follows from equilibrium conditions at vertices [2]. Stavans and Glazier [6] measured internal angles of cells at vertices as a function of the number of sides in a two-dimensional soap froth. They observed significant deviations from the angle 120° that were independent of the length scale. The experimental relation between the average internal angle of n-sided cells $\theta(n)$ and n can be well expressed by the function [23]

$$\theta(n)=120°\left[1+0.5f\left(1-\frac{6}{n}\right)\right], \tag{4}$$

where f is a single fitting parameter between 0 and 1 (e.g., $f=0.3$ for the relation measured in Ref. [6]). For $f=0$ one obtains $\theta(n)=120°$, which corresponds to the lack of deviation from 120° for the average internal angle of n-sided cells. For $f=1$ the formula gives the average internal angle in regular polygons (this behavior is shown as a dotted line in Fig. 11).

In our cellular structures cell edges corresponding to cracks are slightly irregular (see Figs. 1 and 2). In order to measure the angle between cell edges at a given vertex, we replaced each edge near the vertex by a straight segment determined by the least-squares fit to pixels forming the edge and closest to that vertex. The fraction of points f_r of each edge taken into account in the least-squares fit was an adjustable parameter in this procedure. The results obtained for $f_r=0.25$ in our samples are shown in Fig. 10. The dependence of $\theta(n)$ on n in this figure is well expressed by the function (4) with $f=0.15$. We observed that by decreasing f_r the deviations of $\theta(n)$ from 120° decrease, as it is shown in

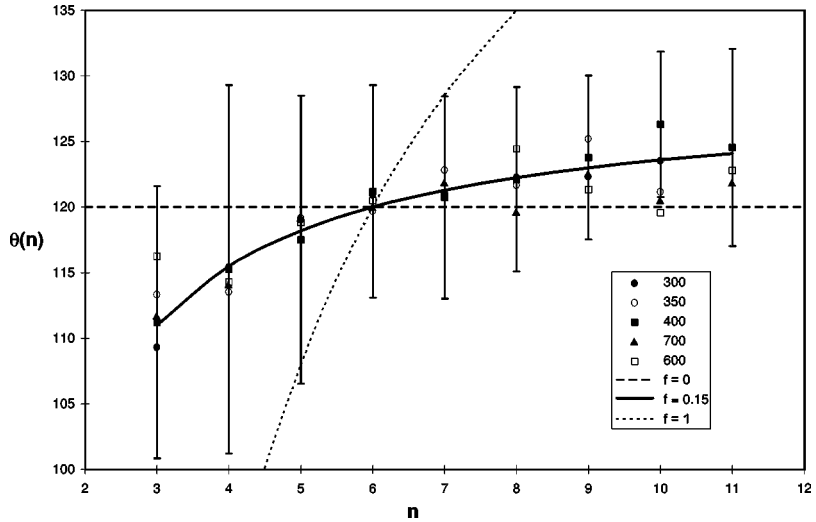

FIG. 10. Average internal angle $\theta(n)$ of n-sided cells as a function of their number of sides n. The angle between cell edges at a vertex was determined by replacing a fraction $f_r=0.25$ of each cell edge near the vertex by a straight segment fitted by the least-squares procedure. The initial temperatures in the water quench test are indicated. The error bars denote a standard deviation and are given for the initial temperature 400 °C. The curves were calculated from Eq. (4).

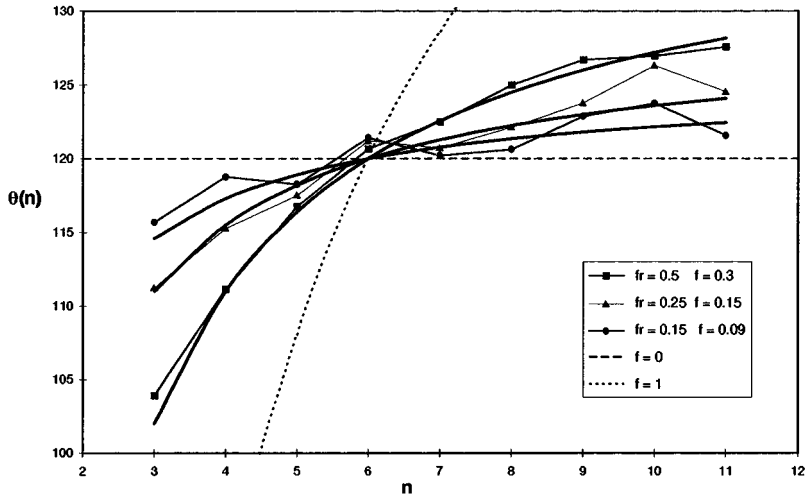

FIG. 11. Average internal angle $\theta(n)$ of n-sided cells as a function of their number of sides n in random cellular structures formed by cracks produced by the thermal shock in ceramic material. The initial temperature in the water quench test was 400 °C. The angle between cell edges at a vertex was determined by replacing a fraction f_r of each cell edge near the vertex by a straight segment fitted by the least-squares procedure. The thin curves connect the results obtained for each value of f_r and are placed to guide the eye. The thick and dashed curves are calculated from Eq. (4). The thick curves fit measured relations. The parameter f for each of these curves is given after the corresponding parameter f_r.

Fig. 11. This property of our crack patterns does not depend on the temperature gradient of the thermal shock. The measured relation between $\theta(n)$ and n for any value of the parameter f_r can be fitted well by the function (4). We could not decrease f_r below 0.15 because of the resolution of our images.

VII. CONCLUSIONS

In this paper we have presented experimental data and an analysis of crack patterns produced by the thermal shock at temperature gradients $\Delta T > \Delta T_c$, where $\Delta T_c \approx 220$ °C, in ceramics used commercially in making tableware. The cracks visible on the surface of a sample partition the surface plane into cells forming a random two-dimensional space-filling cellular structure. We have described topological and geometrical properties of this structure. The results obtained are summarized below.

(i) We observe a large number of cells with five and six sides. The discrete probability density function $P(n)$ is asymmetric and it has the maximum for n between 5 and 6. The average number of cell sides $\langle n \rangle$, is quite close to 6 and the variance of $P(n)$, often used to quantify disorder of random cellular structures, is $\mu_2 = 2.75$.

(ii) The Aboav-Weaire law holds with the value of the parameter $a = 1$, i.e., with a slope equal to 5.

(iii) The number of sides of adjoining cells are correlated in the same way as in many other natural and artificial random space-filling structures with comparable values of μ_2. The two-cell topological correlations show reasonable agreement with the relation derived in Ref. [14] with parameters $a = 1$ and $\mu_2 = 2.75$.

(iv) The probability distributions of normalized areas and side lengths are well represented by the probability density function (3). The values of fitted parameters suggest that there is a correlation between the distribution laws of areas and side lengths. The relations between average values of areas, perimeters, and side lengths also indicate correlations between these quantities.

(v) The radius law (Desch's law) holds, suggesting that the cell energy may be important in the physical model of crack development. The average perimeter of n-sided cells increases linearly with n for $n < 8$.

(vi) We measured angles between cell sides at a vertex approximating cell sides close to the vertex by straight segments obtained by the least-squares fit. The obtained dependence of the average internal angle of n-sided cell on n shows slight deviations from 120°; however, the deviation decreases when cell sides are replaced by straight segments closer and closer to a vertex. This suggests that in the limit the average internal angle of n-sided cells is 120° for all values of n.

Our analysis of crack patterns produced at different temperature gradients of the thermal shock indicates the scaling and uniformity of these patterns. They are indistinguishable apart from a specific scale of length. We conclude that crack patterns considered in this paper are an example of two-dimensional random space-filling cellular structures and follow the general topological and geometric features for these systems. Further investigations are under way to identify the effect of material properties on crack patterns produced by the thermal shock. We are planning to study crack patterns produced by the thermal shock in different ceramics and other materials. It will enhance our current understanding of the crack propagation in materials under thermal stresses.

ACKNOWLEDGMENTS

W.K. thanks the Junta Nacional de Investigação Cientifica e Tecnológica in Portugal for the research grant. We wish to thank the ceramic company SPAL in Portugal for providing us with ceramic samples and Dr. A.L. Ferreira for useful comments.

[1] D. Weaire and N. Rivier, Contemp. Phys. **25**, 59 (1984).
[2] J. Stavans, Rep. Prog. Phys. **56**, 733 (1993).
[3] N. Rivier, Philos. Mag. B **52**, 795 (1985).
[4] S. K. Mendiratta, J. Monteiro, and W. Korneta (unpublished).
[5] I. J. Smalley, Nature (London) **291**, 359 (1981).
[6] J. Stavans and J. A. Glazier, Phys. Rev. Lett. **62**, 1318 (1989).
[7] J. C. Earnshaw and D. J. Robinson, Phys. Rev. Lett. **72**, 3682 (1994).
[8] J. C. Mombach, M. A. Z. Vasconcellos, and R. M. C. de Almeida, J. Phys. D **23**, 600 (1990).
[9] J. A. Glazier, M. P. Anderson, and G. S. Grest, Philos. Mag. B **62**, 615 (1990).
[10] D. A. Aboav, Metallography **3**, 383 (1970).
[11] D. Weaire, Metallography **7**, 157 (1974).
[12] G. Le Caer and R. Delannay, J. Phys. A **26**, 3931 (1993).
[13] M. A. Peshkin, K. J. Strandburg, and N. Rivier, Phys. Rev. Lett. **67**, 1803 (1991).
[14] R. Delannay, G. Le Caer, and M. Khatun, J. Phys. A **25**, 6193 (1992).
[15] J. Lemaitre, A. Gervois, J. P. Troadec, N. Rivier, M. Ammi, L. Oger, and D. Bideau, Philos. Mag. B **67**, 347 (1993).
[16] B. Berge, A. J. Simon, and A. Libchaber, Phys. Rev. A **41**, 6893 (1990).
[17] G. Le Caer and J. S. Ho, J. Phys. A **23**, 3279 (1990).
[18] P. A. Mulheran, Philos. Mag. Lett. **66**, 219 (1992).
[19] D. Weaire, J. P. Kermode, and J. Wejchert, Philos. Mag. B **53**, L101 (1986).
[20] A. G. Evans and T. G. Langdon, Prog. Mater. Sci. **21**, 171 (1976).
[21] F. T. Lewis, Anat. Rec. **38**, 341 (1928).
[22] C. H. Desch, J. Inst. Met. **22**, 241 (1919).
[23] F. Bolton and D. Weaire, Philos. Mag. B **63**, 795 (1991).